Journal of Enzyme Inhibition and Medicinal Chemistry, August 2006; 21(4): 391–397

informa
healthcare

New lipophilic phthalimido- and 3-phenoxybenzyl sulfonates: Inhibition of antigen 85C mycolyltransferase activity and cytotoxicity

ANDREJA KOVAČ[1], ROSALIND A. WILSON[2], GURDYAL S. BESRA[2], METKA FILIPIČ[3], DANIJEL KIKELJ[1], & STANISLAV GOBEC[1]

[1]*Faculty of Pharmacy, University of Ljubljana, Aškerceva 7, 1000 Ljubljana, Slovenia,* [2]*School of Biosciences, The University of Birmingham, Edgbaston, Birmingham B15 2TT, UK, and* [3]*Department of Genetic Toxicology and Cancer Biology, National Institute of Biology, Vecna pot 111, 1000 Ljubljana, Slovenia*

(Received 29 December 2005; in final form 24 February 2006)

Abstract

Four new sulfonates were prepared as potential inhibitors of antigen 85C, a mycolyl transferase involved in the biosynthesis of the mycobacterial cell wall being designed on the basis of the proposed catalytic mechanism and antigen 85C crystal structure. The inhibitors contained a sulfonate moiety, 3-phenoxybenzyl alcohol or *N*-(hydroxyethyl)phthalimide as trehalose mimetics, and an alkyl chain of different length mimicking either the mycolate (α-chain or the mycolic acid (β-branch. One compound displayed promising activity in a mycolyltransferase inhibition assay (compound **2b**, $IC_{50} = 4.3\,\mu M$). The two compounds containing a phthalimide moiety (compounds **3a** and **3b**) showed significant and selective cytotoxicity against the breast cancer cell line MDA-MB231.

Keywords: *Antigen 85C, sulfonate inhibitors, antituberculosis agents, cytotoxicity, anticancer agents, mycolyltransferase*

Introduction

Tuberculosis (TB) is caused by *Mycobacterium tuberculosis* and still remains a leading infectious disease worldwide today. One third of the world population is latently infected with bacteria and there are 8 million new TB cases worldwide with around three million deaths per year. The incidence of the disease is increasing during recent years largely due to HIV infection and also to immigration, increased trade and globalization [1]. Because of the alarming increase of drug-resistant TB and especially multi drug resistant (MDR) TB new and more effective chemotherapeutic agents, also with novel mechanisms of action, are urgently needed [2].

Due to its lipophilicity and low permeability the mycobacterial cell wall is essential for bacterial viability and virulence and an understanding of the biochemistry of mycobacterial cell wall formation is becoming increasingly important in the search for new antimycobacterial drugs [3]. The mycobacterial cell wall core consists of three interconnected macromolecules referred to as the mycolyl-arabinogalactan-peptidoglycan (mAGP) complex [4]. Mycolic acids are long chain α-alkyl-β-hydroxy fatty acids unique to mycobacteria and related genera [5]. They represent the outermost layer of the mAGP complex and are believed to play a crucial role in the stability of the mycobacterial envelope. Mycolic acids are esterified to arabinogalactan or present as free glycolipids, mainly trehalose monomycolate (TMM) and trehalose dimycolate (TDM) [6,7].

Transfer of mycolic acid from one molecule of TMM to another, resulting in TDM and free trehalose is catalyzed by antigen 85 (ag85) complex (Figure 1). Ag 85 complex is a major protein component of

Correspondence: Dr. S. Gobec, Faculty of Pharmacy, University of Ljubljana, Aškerceva 7, 1000 Ljubljana, Slovenia. Tel: 38 6 1 47 69 500, Fax: 386 1 42 58 031. E-mail: gobecs@ffa.uni-lj.si

ISSN 1475-6366 print/ISSN 1475-6374 online
DOI: 10.1080/14756360600703214

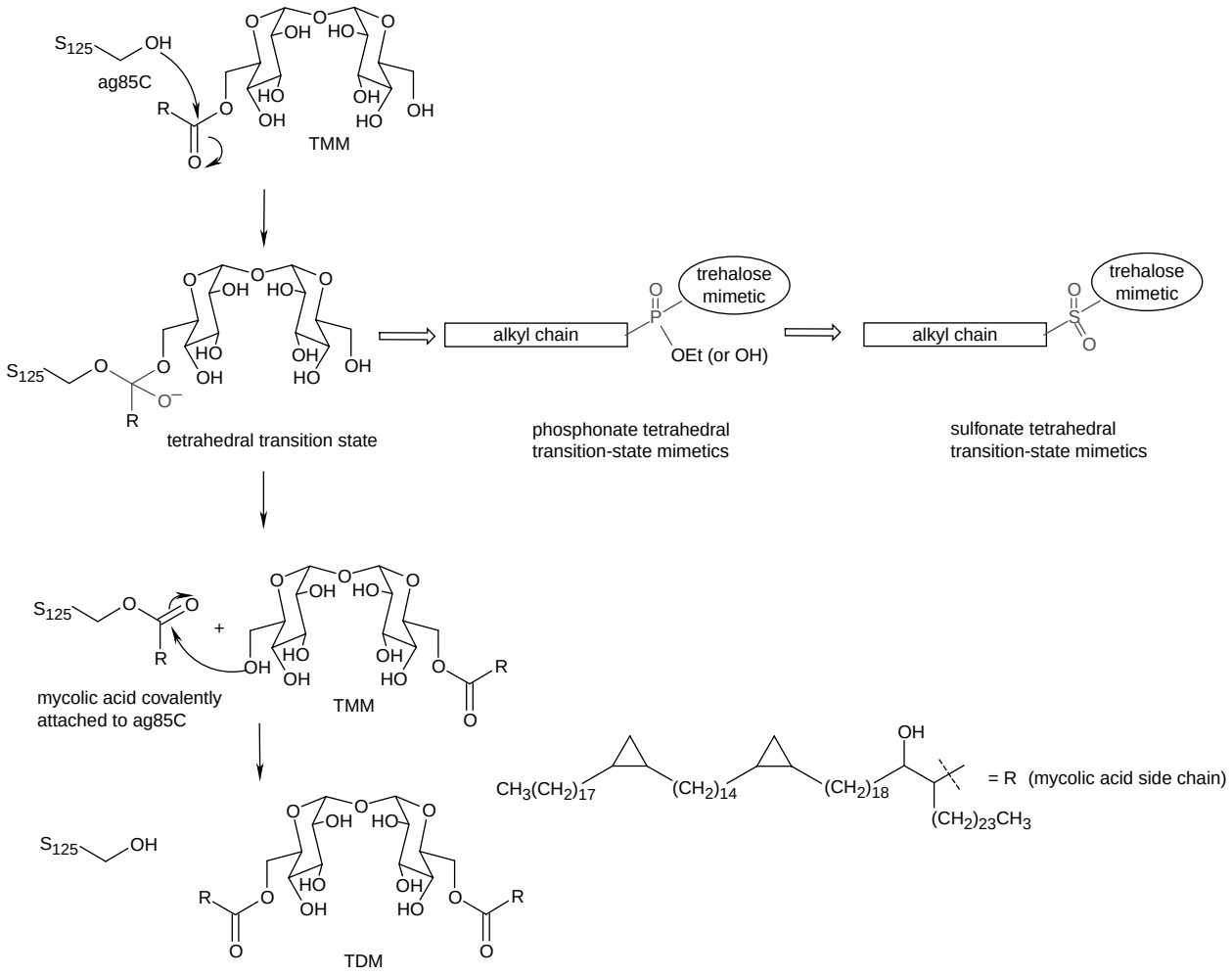

Figure 1. Proposed mechanism of the mycolyl transfer catalyzed by ag85C and design of phosphonate and sulfonate inhibitors.

the mycobacterial cell wall. It is composed of three proteins ag 85A, ag 85B and ag 85C, all of which have mycolyltransferase activity and antigen properties [8]. Beside mycolyltransferase activity, ag 85C is also involved in the transesterification of mycolic acid onto the arabinogalactan. *M. tuberculosis* strain lacking a functional ag 85C gene had 40% less mycolic acids present in the cell wall [9].

The crystal structure of recombinant ag 85C from *M. tuberculosis* reveals a typical α/β-hydrolase polypeptide fold with a catalytic triad formed by Ser 124, Glu 228 and His 260. Near the catalytic triad the enzyme contains a binding site for the carbohydrate moiety with a highly negative electrostatic potential, a hydrophobic tunnel extending towards the core of the protein, which is well suited to accommodate the shorter α-branch of mycolic acid, and a long partially hydrophobic shallow on the surface of the enzyme, supposed to bind the longer β-branch of the mycolic acid [10].

In the first step of the proposed catalytic mechanism, Ser 124 attacks the carboxylate carbon of the TMM molecule to give a mycolyl-enzyme intermediate and free trehalose (Figure 1). In the next step, the 6'-OH group of the second TMM molecule attacks the carboxylate carbon of the acyl-enzyme intermediate, giving TDM. Both steps, acylation and deacylation of the enzyme, proceed via a high-energy tetrahedral transition-state [10].

The importance of TDM to mycobacterial cell wall integrity provides an excellent basis for the development of novel antitubercular drugs. Recently, a series of phosphonates as potential transition-state analogue inhibitors of ag 85C was published [11]. Among them, the most potent inhibitors were compounds containing phthalimido or 3-phenoxybenzyl moiety and lipophilic C_4–C_8 alkyl chain linked together by an ethyl phosphonate moiety to give simplified tetrahedral transition-state analogues (Figure 1, Table I). *N*-Phthalimido and 3-phenoxybenzyl moieties were introduced with the purpose to mimic the trehalose of TMM, while lipophilic alkyl chains could occupy either the mycolate α-chain binding pocket formed by a 21 Å long channel extending through the core of ag 85C protein, or the mycolic acid β-branch binding shallow on the surface of the protein [11].

Table I. Phosphonate inhibitors of the mycolytransferase activity of antigen 85C.

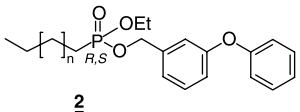 **2**	Inhibition of mycolyltransferase activity⋆	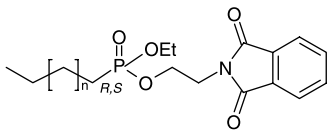	Inhibition of mycolyltransferase activity⋆
n = 1	IC_{50} = 2.01 μM	n = 1	IC_{50} = 50.74 μM
n = 6	IC_{50} = 14.83 μM	n = 6	IC_{50} = 25,67 μM

⋆ Standard deviations are within ± 10% of given values.

Phosphonates and related pentavalent phosphorus species are well established as stable analogues of high-energy transition states with tetrahedral geometry. On the other hand, the use of sulfonate esters for this purpose has, so far, been less investigated, although it was postulated that sulfonates should require a lower desolvation energy than phosphorus analogues which would result in tighter binding and better enzyme inhibition [12]. Based on the structures of our previous inhibitors and preliminary docking studies in the ag 85C active site we designed and synthesized new lipophilic sulfonates as potential transition-state analogues and evaluated their inhibitory activities.

Compounds with the phthalimide scaffold have recently received considerable attention due to their diverse biological activities. There is evidence that certain *N*-substituted phthalimides exhibit potent *in vitro* cytotoxicity against a panel of human tumor cell lines [13–14]. Therefore, we evaluated the compounds with the phthalimide core for their selective cytotoxic activity against some tumor cell lines.

Experimental

Mycolyltransferase assay

Mycolyltransferase assays were performed by resuspending 62.5 μg of TMM in 50 μL of 0.1 M potassium phosphate (pH 7.5) and 10 mM DTT and the mixture sonicated for 15 min. To this mixture was added 100 μg of enzyme and [^{14}C]trehalose (0.25 μCi, 30.4 mCi/mmol, Amersham) along with the inhibitor in a final volume of 200 μL and the contents incubated at 37°C for 30 min. The reaction was stopped by adding 3 mL of $CHCl_3/CH_3OH$ (2:1) and 300 μL of water. This mixture was vortexed, centrifuged and the upper aqueous phase was discarded. The lower organic layer was washed twice using 0.5 mL of $CHCl_3/CH_3OH/H_2O$ (3:47:48) and finally dried under a stream of nitrogen. The resulting organic extractable material containing the products of the mycolyltransferase reaction was resuspended in 100 μL of $CHCl_3/CH_3OH$ (2:1). A 50 μL aliquot was dried prior to the addition of 5 mL of scintillation fluid and counted. Thin-layer chromatography (TLC)-autoradiography of the organic extractable products was performed with silica gel TLC plates using the solvent system $CHCl_3/CH_3OH/NH_4OH$ (80:20:2). TDM and TMM standards were visualised by spraying with 10% α-naphthol in 5% sulfuric acid in ethanol and heating at 110°C.

In vitro cytotoxicity

Cytotoxicity for phthalimide-based compounds **3a** and **3b** was determined with 3-(4,5-dimethylthiazol-2-yl)-2,5-diphenyltetrazolium bromide (MTT) according to Mosmann [20] with minor modifications. This assay measures the conversion of MTT to insoluble formazan by the mitochondrial dehydrogenase enzymes of living cells. The *in vitro* cytotoxicity was evaluated against three human tumour cell lines-MDA-MB231 (breast cancer), 103H (large cell lung cancer) and HepG2 (human hepatoma) and HUVEC cells (human endothelial cells) that represented normal cells.

MDA-MB-231 cells were cultivated in L-15 (Sigma, St. Louis, USA) medium, 103H cells in RPMI 1640 (Sigma, St. Louis, USA), HepG2 cells in William's medium E (Sigma, St. Louis, USA) and HUVEC in EMEM with nonessential amino acids (Sigma, St. Louis, USA). All the media were supplemented with 10% foetal bovine serum, 2 mM L-glutamine and 100 U/ml penicillin/streptomycin. The cells were incubated at 37°C in humidified atmosphere with 5% CO_2.

Cells were seeded in 200 μL of growth media in Corning 96-well microtiter plates at 6,000 cells per well (MDA-MB231), 9,000 cells per well (103H), 25,000 cells per well (HepG2) and 2,500 cells per well (HUVEC). On the next day the medium was replaced by complete growth medium containing 10^{-5} M test compound and the cells were incubated for 24 or 48 h (control cells were incubated in complete medium containing vehicle: 0.1% DMSO). The cells were then washed twice with PBS and the medium was replaced by fresh complete growth medium containing MTT (final concentration 0.5 mg/ml). After 3 h the medium was removed and the resulting formazan crystals

dissolved in DMSO. The absorbance (A) of each well was measured at 570 nm (reference filter 690 nm) using an ELISA microplate reader. Survival (viability) was determined by comparing absorbance in the wells containing treated cells to that of untreated cells. Five replicates were measured for each concentration.

Molecular docking

Automated docking was used to locate the potential binding orientation of inhibitors within the active site of ag85C. The Genetic algorithm method implemented in the program AutoDock 3.0 was employed [21]. The structures of inhibitors were prepared using HyperChem 7.5 (HyperChem, version 7.5 for Windows. Hypercube, Inc.: Gainesville, FL, 2002). Crystal structure of Ag85C was retrieved from the RCSB protein data base (PDB entry 1VA5) and all ligands and water molecules were removed. Polar hydrogen atoms were added and Kollman charges, [22] atomic solvation parameters and fragmental volumes were assigned to the protein using AutoDock Tools (ADT). For docking calculations, Gasteiger-Marsili partial charges [23] were assigned to the ligands and nonpolar hydrogen atoms were merged. All torsions were allowed to rotate during docking. The grid map, which was centred at Ser-124 of the protein, was generated with the auxiliary program AutoGrid. The grid dimensions were large enough to cover the inhibitors and the enzyme's active site. Lennard-Jones parameters 12-10 and 12-6, supplied with the program, were used for modeling H-bonds and van der Waals interactions, respectively. The distance-dependent dielectric permittivity of Mehler and Solmajer [24] was used for the calculation of the electrostatic grid maps. For all ligands, random starting points, random orientation, and torsions were used. The translation, quaternion, and torsion steps were taken from default values in AutoDock. The Lamarckian genetic algorithm and the pseudo-Soils and Wets methods were applied for minimization, using default parameters. The number of docking runs was 100, the population in the genetic algorithm was 250, the number of energy evaluations was 500,000, and the maximum number of iterations was 27,000.

Results and discussion

New sulfonates **2a**–**b** and **3a**–**b** were prepared from the sulfonyl chlorides **1a** or **1b** and 3-phenoxybenzyl alcohol or *N*-(2-hydroxyethyl)phthalimide in the presence of excess triethylamine in dioxane (Scheme 1). The target sulfonates were obtained in good yields (75–90%) after purification by column chromatography.

In the series of new sulfonates two different alcohols, *N*-(2-hydroxyethyl)phthalimide and 3-phenoxybenzyl, were used as mimetics of trehalose of TMM. They were coupled with alkylsulfonyl chlorides having chain lengths of C_4 and C_8 atoms. Hydrophobic alkyl moieties were introduced to mimic either the α-chain or β-branch of the mycolic acid. Different chain lengths were chosen to study the influence of hydrophobicity and size of target compounds on their inhibitory activity. The compounds listed in Table II were assayed *in vitro* for their inhibition of recombinant *M. tuberculosis* antigen 85C mycolyltransferase activity [8].

Compound **2b** containing a 3-phenoxybenzyl moiety and C_8 alkyl chain showed very promising mycolyltransferase activity with an IC_{50} in the low micromolar range ($IC_{50} = 4.3\,\mu M$). The other 3-phenoxybenzyl alcohol derivative (**2a)** and *N*-(2-hydroxyethyl)phthalimide derivatives (**3a–b)** were all inactive. Comparison of the results with the data for the series of structurally related phosphonates leads to the conclusion that the replacement of phosphonate with sulfonate moiety does not influence the mycolyltransferase inhibitory activity in the 3-phenoxybenzyl series containing medium size alkyl chain of 8 carbons. If the alkyl chain is shorter

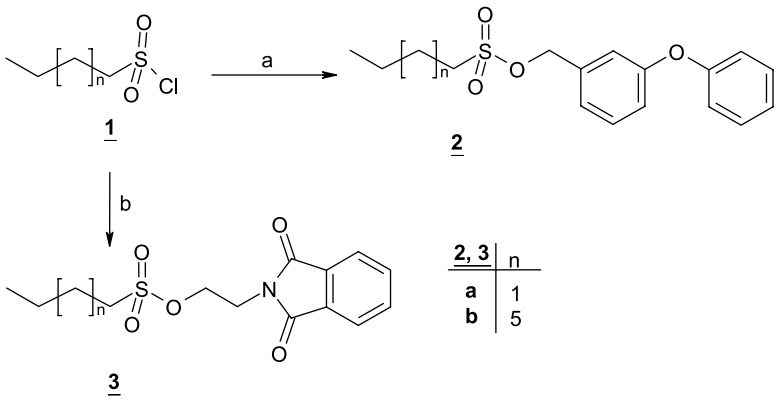

Scheme 1. Reagents and conditions. (a) 3-phenoxybenzyl alcohol, TEA, dioxane, 0°C, 1h, then rt, 24h; (b) *N*-(2-hydroxyethyl)phthalimide, TEA, dioxane, 0°C, 1h, then rt, 24h.

Table II. Inhibition of ag85C mycolyltransferase activity.

Compound	Inhibition of mycolyltransferase activity
2a	NI*
2b	$IC_{50} = 4.3 \pm 4\,\mu M$
3a	NI*
3b	NI*

Results represent means of three experiments ± standard deviation.
*No inhibition.

or *N*-(2-hydroxyethyl)phthalimide moiety is introduced into the molecule the compounds are no longer active.

Docking experiments predicted that the 3-phenoxybenzyl substituent of compound **2b** would locate in the trehalose binding pocket and the sulfonate moiety would be oriented in the vicinity of Ser124. The alkyl chain would accommodate in the mycolate α-chain binding channel extending through the core of the protein (Figure 2). A similar binding mode was recently observed in the crystal structure of the substrate analog octylthioglucoside co-crystalized with antigen 85C [15].

The best known phthalimide-containing compound is undoubtedly thalidomide (*N*-α-phthalimido-glutarimide), a sedative which was removed from the market almost 50 years ago due to its teratogenicity. However, after withdrawal of thalidomide its numerous desirable effects have been discovered. It posseses immunomodulatory, anti-inflammatory, cytotoxic and antiangiogenic activity [16–19]. Compounds with the phthalimide core are thus highly interesting as potential anticancer agents [13–14]. We evaluated *N*-(2-hydroxyethyl)phthalimide derivatives (**3a**–**b)** for their *in vitro* cytotoxicity against four different cell lines. Three of them were human tumor cell lines - MDA-MB231 (breast cancer), 103H (large cell lung cancer) and HepG2 (human hepatoma), while HUVEC cells (human umbilical vein endothelial cells) were used as a non-tumor cells. The exponentially growing cells were exposed to the compounds (at 10^{-5} M) for 24 h or 48 h and cytotoxic effect was determined by a tetrazolium-based colorimetric assay (MTT assay) [20]. The results are summarized in Table III. Both compounds showed significant

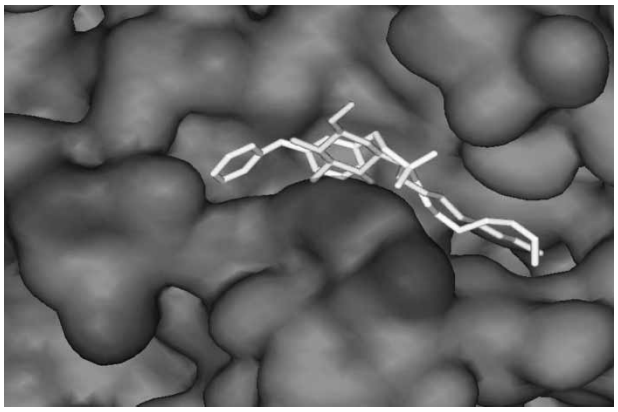

Figure 2. Superimposition of the computer model of compound **2b** (in white) on the X-ray structure of octylthioglucoside (in gray) bound to ag 85C (PDB entry 1VA5). The 3-phenoxybenzyl substituent of compound **2b** is located in the trehalose binding pocket. The alkyl chain is accommodated in the mycolate α-chain binding channel extending through the core of ag85C.

cytotoxicity against the breast cancer cell line MDA-MB231. After 24 hours of exposure they reduced viability of MDA-MB231 cells by about 30%. With prolongation of the exposure from 24 to 48 hours, compound **3a** reduced cell viability by nearly 70%, while compound **3b**, did not further reduce the viability of MDA-MB231 cells. The viability of 103H cells was transiently reduced only by compound **3b.** After 24 hours of exposure, viability was reduced by about 30% while after 48 h of exposure the cells recovered and the viability did not differ from that of the control cells. None of the compounds was cytotoxic to the HepG2 cell line and HUVEC cells. These results indicate selective cytotoxicity against the tumor cell line MDA-MB231. Phthalimide-based compounds **3a** and **3b** are thus highly interesting for further investigations as potential anticancer agents.

Chemistry

All reactions were carried out under dry conditions and with magnetic stirring. Chemicals were purchased from Acros and used without further purification. Solvents were used without purification or drying,

Table III. Cytotoxic activity of new phthalimide derivatives **3a** and **3b**.

Compound (c=10^{-5} M)	Cytotoxicity (viability %)*							
	HepG2		MDA-MB231		103H		Huvec	
	24 h	48 h	24 h	48 h	24 h	48 h	24 h	48 h
3a	NI**	NI**	69 ± 7	33 ± 10	NI**	NI**	NI**	NI**
3b	NI**	NI**	68 ± 5	65 ± 9	69 ± 4	NI**	NI**	NI**

Results represent means of five experiments ± standard deviation.
* % of viable cells in exposed culture compared to non-exposed control.
** No inhibition.

unless otherwise stated. Reactions were monitored using analytical TLC plates (Merck, silica gel 60 F_{254}) with sulphuric acid staining. Silica gel grade 60 (70–230 mesh, Merck) was used for column chromatography. ^{1}H NMR spectra were recorded on a Bruker Avance DPX 300 instrument at 300.13 MHz with tetramethylsilane as an internal standard. Mass spectra were obtained with a VG-Analytical Autospec Q mass spectrometer with EI or FAB ionization (MS Centre, Jožef Stefan Institute, Ljubljana). IR spectra were recorded on a Perkin-Elmer FTIR 1600 spectrometer. Elemental analyses were performed by the Department of Organic Chemistry, Faculty of Chemistry and Chemical Technology, Ljubljana, on a Perkin Elmer elemental analyzer 240 C. Melting points were determined using a Reichert hot-stage microscope and are uncorrected.

*General procedure for the synthesis of compounds **2a–b** and **3a–b***. Triethylamine (3.6 mmol) was added to a stirred solution of the alcohol (3-phenoxybenzyl alcohol or *N*-(2-hydroxyethyl)phthalimide) (2.0 mmol) in dioxane and the mixture was cooled on an ice bath to 0°C. 1-Butanesulfonyl chloride or 1-octanesulfonyl chloride (**1**) (2.4 mmol) was added dropwise over a period of 30 min and the reaction mixture then stirred overnight at room temperature. After 24 h, diethyl ether added and the resulting precipitate was filtered off. The residual solution was concentrated in vacuo and purified by column chromatography on silica gel (eluent: CH_2Cl_2).

*1-(3-Phenoxy)benzyl 1-butanesulfonate (**2a**)*. Yield: 85% (oil); IR (KBr) 692, 830, 932, 1164, 1259, 1355, 1448, 1488, 1586, 2876, 2962 cm^{-1}; ^{1}H NMR (300 MHz, $CDCl_3$): δ 0.90–1.00 (t, 3H, J = 6.8 Hz, CH_3CH_2), 1.35–1.50 (m, 2H, CH_3CH_2), 1.75–1.90 (m, 2H, $CH_2CH_2CH_2$), 3.00–3.10 (m, 2H, $CH_2CH_2SO_2O$), 5.20 (s, 2H, OCH_2Ar), 7.00–7.40 (m, 9H, ArH). FAB MS *m/z* 320 $[M + H]^+$. Anal. Calcd. for $C_{17}H_{20}O_4S$: C, 63.75; H, 6.25. Found: C, 64.02; H, 6.44%.

*1-(3-Phenoxy)benzyl 1-octanesulfonate (**2b**)*. Yield: 75% (oil); IR (KBr) 692, 834, 931, 1165, 1259, 1357, 1448, 1488, 1586, 2856, 2927 cm^{-1}; ^{1}H NMR (300 MHz, $CDCl_3$): δ 0.90 (t, 3H, J = 6.8 Hz, CH_3CH_2), 1.25–1.45 (m, 10H, $CH_3(CH_2)_5$), 1.78–1.88 (m, 2H, $CH_2CH_2SO_2O$), 3.01–3.08 (m, 2H, $CH_2CH_2SO_2O$), 5.20 (s, 2H, OCH_2Ar), 7.00–7.40 (m, 9H, ArH). FAB MS *m/z* 376 $[M + H]^+$. Anal. Calcd. for $C_{21}H_{28}O_4S$: C, 67.02; H, 7.45. Found: C, 67.02; H, 7.66%.

*2-(1,3-Dioxo-1,3-dihydro-2H-isoindol-2-yl)ethyl 1-butanesulfonate (**3a**)*. Yield: 80%; m.p.: 93–94 °C; IR (KBr) 600, 719, 824, 978, 1026, 1173, 1336, 1399, 1469, 1723, 1777, 2968, 3479 cm^{-1}; ^{1}H NMR (300 MHz, DMSO-d_6): δ 0.78 (t, 3H, J = 7.4 Hz, CH_3CH_2), 1.22–1.35 (m, 2H, CH_3CH_2), 1.54–1.61 (m, 2H, $CH_2CH_2CH_2$), 3.20–3.30 (m, 2H, $CH_2CH_2SO_2O$), 3.92 (t, 2H, J = 5.28 Hz, $SO_2OCH_2CH_2N$), 4.40 (t, 2H, J = 5.28 Hz, $SO_2OCH_2CH_2N$), 7.80–7.95 (m, 4H, ArH). FAB MS *m/z* 312 $[M + H]^+$. Anal. Calcd. for $C_{14}H_{17}NO_4S$: C, 54.01; H, 5.50; N, 4.50. Found: C, 54.05; H, 5.81; N, 4.25%.

*2-(1,3-Dioxo-1,3-dihydro-2H-isoindol-2-yl)ethyl 1-octanesulfonate (**3b**)*. Yield: 78%; m.p.: 53–55 °C; IR (KBr) 576, 722, 809, 862, 919, 990, 1167, 1250, 1350, 1470, 1710, 2920 cm^{-1}; ^{1}H NMR (300 MHz, DMSO-d_6): δ 0.85 (t, 3H, J = 7.0 Hz, CH_3CH_2), 1.10–1.32 (m, 10H, $CH_3(CH_2)_5$), 1.49–1.61 (m, 2H, $CH_2CH_2SO_2O$), 3.21–3.28 (m, 2H, $CH_2CH_2SO_2O$), 3.92 (t, 2H, J = 4.6 Hz, $SO_2OCH_2CH_2N$), 4.40 (t, 2H, J = 4.6 Hz, $SO_2OCH_2CH_2N$), 7.80–7.94 (m, 4H, ArH). FAB MS *m/z* 368 $[M + H]^+$. Anal. Calcd. for $C_{18}H_{25}O_4S$: C, 58.83; H, 6.86; N, 3.81. Found: C, 58.71; H, 6.76; N, 3.81%.

References

[1] World Health Organisation [internet]., Tuberculosis: Fact Sheet No. 104; 2005-[cited 2005 Apr]; Available from: http://www.who.int/mediacentre/factsheets/fs104/en/

[2] Zhang Y, Amzel LM. Tuberculosis drug targets. Curr. Drug Targ. 2002;3:131–154.

[3] Kremer L, Besra GS. Current status and future development of antitubercular chemotherapy. Exp. Opin. Invest. Drugs 2002;11:1033–1049.

[4] Brennan PJ, Nikaido H. The envelope of mycobacteria. Ann Rev. in Biochem. 1995;64:29–63.

[5] Barry CE, Lee RE, Mdluli K, Sampson AE, Schroeder BG, Slayden RA, Yuan Y. Mycolic acids: Structure biosynthesis and physiological functions. Progr Lipid Res. 1998;37:143–179.

[6] Besra GS, Khoo K-H, McNeil MR, Dell A, Morris HR, Brennan PJ. A new interpretation of the structure of the mycolyl arabinogalactan complex of mycobacterium tuberculosis as revealed through characterization of oligoglycosylalditol fragments by fast-atom-bombardment mass-spectrometry and H-1 nuclear-magnetic-resonance spectroskopy. Biochemistry 1995;34:4257–4266.

[7] McNeil MR, Daffe M, Brennan PJ. Location of the Mycolyl Ester Substituents in the Cell walls of mycobacteria. J. Biol. Chem. 1991;266:13217–13223.

[8] Belisle JT, Vissa VD, Sievert T, Takayama K, Brennan PJ, Besra GS. Role of mayor antigen of *Mycobacterium tuberculosis* in Cell Wall Biogenesis. Science 1997;276:1420–1422.

[9] Jackson M, Raynaud C, Laneelle MA, Guilhot C, Laurent-Winter C, Ensergueix D, Gicquel B, Daffe M. Inactivation of the antigen 85C gene profoundly affects the mycolate content and alters the permeability of the *Mycobacterium tuberculosis* cell envelope. Molec. Microbiol. 1999;31:1573–1578.

[10] Ronning DR, Klabunde T, Besra GS, Vissa VD, Belisle JT, Sacchettini JC. Crystal structure of the secreted form of antigen 85C reveals potential target for mycobacterial drugs and vaccines. Nature Struct. Biol. 2000;7:141–146.

[11] Gobec S, Plantan I, Mravljak J, Wilson RA, Besra GS, Kikelj D. Phosphonate inhibitors of antigen 85C, a crucial enzyme

involved in the biosynthesis of the Mycobacterium tuberculosis cell wall. Bioorgan. Med. Chem. Lett. 2004;14:3559–3562.

[12] Yang K-W, Golich FC, Sigdel TK, Crowder MW. Phosphinate, sulfonate, and sulfonamidate dipeptides as potential inhibitors of *Escherichia coli* aminopeptidase N. Bioorgan. Med. Chem. Lett. 2005;15:5150–5153.

[13] Hall IH, Wong OT, Scovill JP. The citotoxicity of *N*-pyridinyl and *N*-quinolinyl substituted derivatives of phthalimide and succinimide. Biomed. Pharmacother. 1995;5:251–258.

[14] Hall IH, Wong OT, Chapman JM. Citotoxicity of imides-N-alkyl semicarbazones, thiosemicarbazones, acetylhydrazones and related derivatives. Anti-Cancer Drugs 1995; 6:147–153.

[15] Ronning DR, Vissa V, Besra GS, Belisle JT, Sacchettini JC. Mycobacterium tuberculosis antigen 85A and 85C structures confirm binding orientation and conserved substrate specificity. J. Biol. Chem. 2004;279: 36771–36777.

[16] Peuckmann V, Fisch M, Bruera E. Potential novel uses of thalidomide. Drugs 2000;60:273–292.

[17] Hashimoto A. Novel biological response modifiers derivated from thalidomide. Curr. Med. Chem. 1998;5:163–178.

[18] Calabrese L, Fleischer AB. Thalidomide: Current and potential clinical application. Amer. J. Med. 2000;108:487–495.

[19] Fanelli M, Sarmiento R, Gattuso D, Carillio G, Capaccetti B, Vacca A, Roccaro AM, Gasparini G. Thalidomide: A new anticancer drug? Exp. Opin. Investig. Drugs 2003;12: 1211–1225.

[20] Mosmann T. Rapid colorimetric assay for cellular growth and survival — application to proliferation and cyto-toxicity assays. J. Immunol. Meth. 1983;65:55–63.

[21] Morris GM, Goodsell DS, Halliday RS, Huey R, Hart WE, Belew RK, Olson AJ. Automated docking using a Lamarckian genetic algorithm and an empirical binding free energy function. J. Comput. Chem. 1998;19:1693–1662.

[22] Weiner SJ, Kollman PA, Case DA, Singh UC, Ghio C, Alagona G, Profeta S, Weiner P. A new force-field for molecular mechanical simulation of nucleic acids and proteins. J. Amer. Chem. Soc. 1984;106:765–784.

[23] Gasteiger J, Marsili M. Iterative partial equalization of orbital electronegativity — a rapid access to atomic charges. Tetrahedron 1980;36:3219–3228.

[24] Mehler EL, Solmajer T. Electrostatic effects in proteins-comparison of dielectric and charge models. Prot. Eng. 1991;4:903–910.